Quaternary Geochronology 22 (2014) 72–84

Contents lists available at ScienceDirect

Quaternary Geochronology

journal homepage: www.elsevier.com/locate/quageo

Research paper

Defining optimal sample size, sampling design and thresholds for dendrogeomorphic landslide reconstructions

Christophe Corona [a,b,*], Jérôme Lopez Saez [c], Markus Stoffel [b,d]

[a] Centre National de la Recherche Scientifique (CNRS) UMR6042 Geolab, 4 rue Ledru, F-63057 Clermont-Ferrand Cedex, France
[b] University of Berne, Institute of Geological Sciences, Dendrolab.ch, Baltzerstrasse 1+3, CH-3012 Berne, Switzerland
[c] Institut national de Recherche en Sciences et Technologies pour l'Environnement et l'Agriculture (Irstea), UR EMGR, 38402 St-Martin-d'Hères cedex, France
[d] University of Geneva, Institute for Environmental Sciences, Climatic Change and Climate Impacts, 7 route de Drize, CH-1227 Carouge, Geneva

ARTICLE INFO

Article history:
Received 11 July 2013
Received in revised form
3 February 2014
Accepted 18 February 2014
Available online 6 March 2014

Keywords:
Tree ring
Dendrogeomorphology
Mass movement
Sampling design
Sample size
Spatial analysis

ABSTRACT

Trees affected by mass movements record the evidence of geomorphic disturbance in their growth-ring series, and thereby provide a precise geochronological tool for the reconstruction of past process activity. At the tree scale, identification of past mass movements was typically based on the presence of growth anomalies and focused on the presence of scars, tilted or buried trunks, as well as on apex decapitation. In terms of sampling strategy, however, clear guidelines have been largely missing. Most previous work was based either on the sampling of visibly disturbed trees irrespective of their position at the study site or on the systematic sampling of trees evenly distributed along transects. Based on a dense dataset of 323 trees growing on an active landslide body, this study aims at defining guidelines for future tree-ring sampling of landslides. Using random extractions of trees and iterative mapping, we investigate subsets of the full tree-ring sample to define optimal sampling strategy, sample depth and trees for the development of frequency maps of landslide reactivations. We demonstrate that (i) the sampling of 50–100 trees can be sufficient to obtain satisfactory results on landslide frequency without including noise to the dendrogeomorphic record; (ii) increasing growth disturbance thresholds should be adjusted to sample size and are preferable to fixed values; (iii) an even distribution of sampled trees is crucial to increase the reliability of frequency maps, even more so if the reconstruction is based on small sample sizes; and that (iv) the selection of the most frequently disturbed trees is key to reduce uncertainties in the frequency maps. The optimization of sample sizes and the adjustment of sampling strategy will not only facilitate fieldwork and render analyses and interpretation more reliable, but will also ultimately allow reconstruction of time series of past mass movements with reasonable temporal efforts and excellent cost-benefit ratios.

1. Introduction

Dendrochronology is one of the most accurate and precise dating methods in geochronology (Stahle et al., 2003), and has also been demonstrated to represent a valuable recorder of mass movement activity (Alestalo, 1971; Stoffel et al., 2010, 2013; Stoffel and Corona, 2014). Growth-ring series of disturbed trees have been used widely for the reconstruction of time series of various types of geomorphic (e.g., McAuliffe et al., 2006; Stoffel et al., 2008, 2012; Bollschweiler et al., 2009; Lopez Saez et al., 2012a,b; Osterkamp et al., 2012), hydrologic (St. George and Nielsen, 2002; Ballesteros et al., 2011a,b; Stoffel and Wilford, 2012), and geologic (Jacoby et al., 1988; Salzer and Hughes, 2007; Baillie, 2008; Bekker, 2010; Stoffel et al., 2005, 2011; Corona et al., 2012) processes. In addition, dendrogeomorphic data has been demonstrated to permit an accurate mapping of both past events and return periods (e.g. Stoffel et al., 2005; Corona et al., 2010; Lopez Saez et al., 2012b).

Recent advances in dendrogeomorphic research have demonstrated that an appropriate sampling design and size (Schneuwly-Bollschweiler et al., 2013; Trappmann et al., 2013) is indeed key to improve reliability as well as traceability of results, even more so if data is used for hazard assessments and disaster risk reduction. To date, sampling strategies focused typically on trees with visible growth defects and related growth disturbances (GD) in the tree-ring record. Guidelines for the tree-ring sampling of tilted or

* Corresponding author. Centre National de la Recherche Scientifique (CNRS) UMR6042 Geolab, 4 rue Ledru, F-63057 Clermont-Ferrand Cedex, France.
E-mail address: christophe.corona@univ-bpclermont.fr (C. Corona).

http://dx.doi.org/10.1016/j.quageo.2014.02.006
1871-1014/

buried trunks, impact scars or trees with decapitated apices were defined at the tree scale (Stoffel and Bollschweiler, 2008) and different types and intensities of reactions have been given different weight in reconstructions (see Stoffel and Corona, 2014 for a recent review). In addition, recent work has shown quite clearly that tree selection as well as an adequate mixture of tree species and age classes are in fact fundamental for the reconstruction of well-balanced and minimally biased time series of past mass-movement activity (Trappmann and Stoffel, 2013; Stoffel et al., 2013; Corona et al., 2012).

Yet, at the slope scale, no clear rules exist as of today on how and where to realize tree-ring sampling (in terms of sampling design) and on how many samples to take (i.e. sample size). A vast majority of past studies was based on either random sampling of trees with visible growth defects (Stoffel et al., 2010; Corona et al., 2010) or on the systematic sampling along transects (Schneuwly and Stoffel, 2008; Trappmann and Stoffel, 2013; Schläppy et al., 2013). In addition, the influence of the spatial distribution of sampled trees on the quantity and quality of mass-movement reconstructions has never been tested objectively, but has, at best, been considered as a subjective exclusion criterion in past work (Lopez Saez et al., 2012b, 2013; Schneuwly-Bollschweiler et al., 2013).

As a logical consequence of largely differing sample design and size, considerably varying thresholds have been suggested in the past to distinguish signal (events) from noise (non-events). Some authors have dated past mass-movement activity based on one single GD in just one tree, whereas others only accepted event years where 40% of all trees sampled showed GD (Butler et al., 1987; Butler and Sawyer, 2008). Differences in thresholds will not only yield substantially different times series of events, but have also given rise to repeated and contentious discussions on the value, accuracy and completeness of dendrogeomorphic dating and, thus, call quite clearly for the definition of more objective standards and guidelines on how and where to sample and on how to interpret results.

In this paper, we therefore propose a more objective means for the determination of the best sampling design and the definition of optimal sample sizes and thresholds. Based on an event chronology derived from a large set of trees affected by landslide reactivations in the southern French Alps, we (i) test different subsets of trees and (ii) calibrate thresholds for sample size and index values (i.e. percentage of responses relative to the number of trees alive in a given year) to obtain optimal signal-to-noise ratios in reconstructions. We then (iii) characterize the optimal spatial configuration of trees to be sampled on the landslide body using random bootstrap extraction. In a final step, we (iv) characterize trees (in terms of age, number of GD, frequency of GD) involved in each optimal subset so as to facilitate the selection of optimal trees in future reconstructions.

2. Study site

The Pra Bellon landslide (44°25′ N., 6°37′ E., Fig. 1a) is located in the Riou-Bourdoux catchment, a tributary of the Ubaye River located on the N-facing slopes of the Barcelonnette basin (Alpes de Haute-Provence, France). The Riou-Bourdoux catchment has been

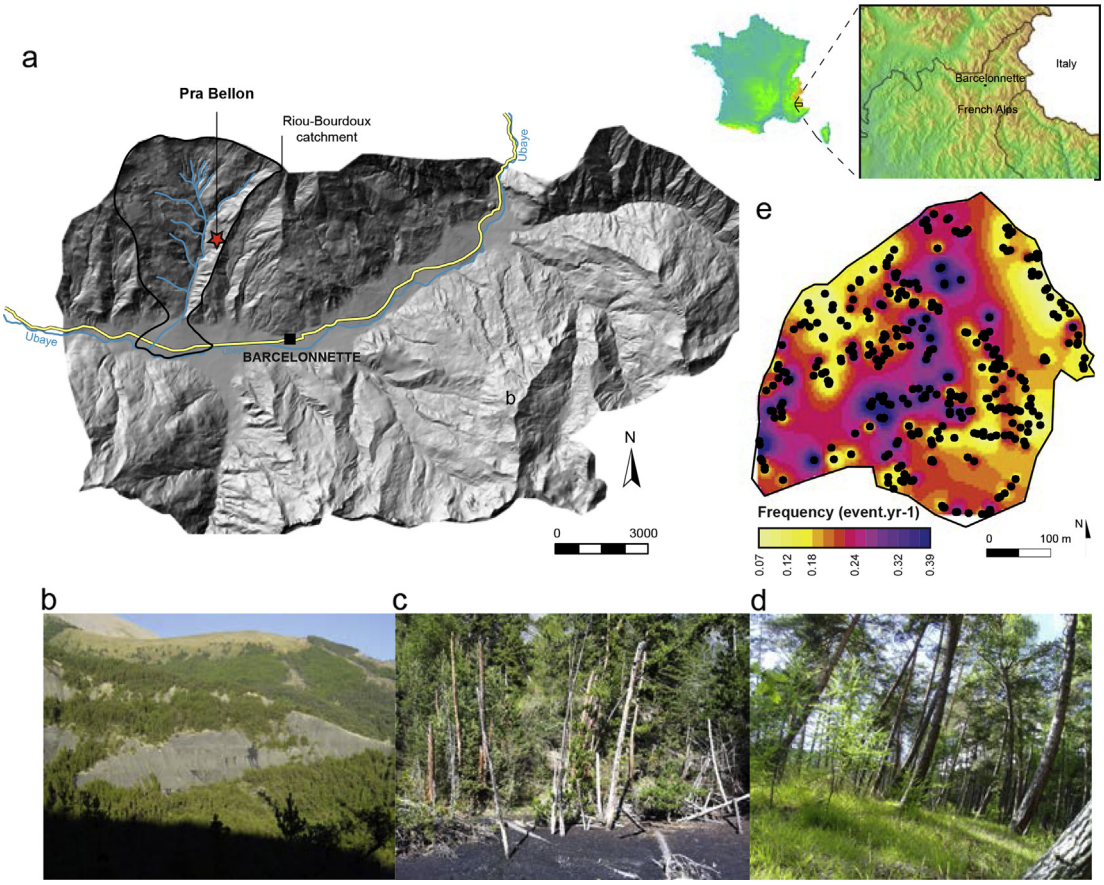

Fig. 1. (a) The Pra Bellon landslide is located in the Ubaye valley (southern French Alps), near the village of Saint-Pons. (b) View of the two mains scarps (SC1 and SC2) of the landslide body. (c) Buried and (d) tilted Mountain pine (*Pinus uncinata*) trees were used to reconstruct past landslide activity. (e) Interpolated frequency maps for the sampled area of the Pra Bellon landslide computed from growth disturbances observed in 323 trees.

Table 1
Overview of past dendrogeomorphic studies of landslide processes and approaches (thresholds) used.

Authors	Year	Localisation	Country	Number of landslides	Species	Sample depth	Period	Nb of growth disturbances	Minimal index value	Number of landslide reactivations
McGee	1893	Tenessee	USA	Unknown	Not precised	Unknown	1812	Not computed	Not computed	Not computed
Fuller	1912	Mississipi	USA	Unknown	Not precised	Unknown	1811 −1812	Not computed	Not computed	Not computed
Shroder	1978	Utah	USA	1	*Picea engelmannii,Pinus flexilis, Pseudotsuga menziesii*	260	1781 −1958	Not computed	4%	14
Terasme	1975	Ontario	Canada	1	Not precised	Unknown	Unknown	Not computed	Not computed	Not computed
Reeder	1979	Alaska	USA	1	Not precised	Unknown	Unknown	Not computed	Not computed	Not computed
Palmquist et al.	1981	Wyoming	USA	1	Not precised	Unknown	Unknown	Not computed	Not computed	Not computed
Jensen	1983	Wyoming	USA	1	Not precised	Unknown	Unknown	Not computed	Not computed	Not computed
Bégin and Filion	1985	Quebec	Canada	1	*Picea abies*	52	1785 −1933	Not computed	Not computed	8
Bégin and Filion	1988	Quebec	Canada	7	*Picea abies*	Not precised	1818	Not computed	Not computed	1
Braam et al.	1987	Alps	France	2	*Pinus uncinata*	56	1890 −1980	Not computed	7-17%	24
Van Asch and Van Steijn	1991	Alps	France	1	Not precised	65	1900 −1982	Not computed	10%	15
Williams et al.	1992	Washington	USA	4	Not precised	Unknown		Not computed	Not computed	Not computed
Flemming and Johnson	1994	Ohio	USA	1	Not precised	Unknown	1958	Not computed	Not computed	Not computed
Astrade et al.	1998	Alps	France	1	*Pinus sylvestris*	41	1923 −1994	Not computed	10%	9
Corominas and Moya	1999	Pyrenees	Spain	7	Not precised	250	1926 −1995	Not computed	30	35
Fantucci and Sorriso-Valvo	1999	Calabria	Italy	1	*Quercus pubescens, Pinus nigra*	38	1845 −1995	Not computed	Not computed	1
Carrara	2003	Wyoming	USA	1	*Pseudotsuga menziesii*	13	1865	Not computed	Not computed	1
Carrara and O'neill,	2005	Montana	USA	3	*Pseudotsuga menziesii, Pinus contorta, Pinus flexilis, Abies lasiocarpa*	32	1880 −1992	Not computed	25%	20
Stefanini	2004	Appenines	Italy	1	*Quercus cerris*	24	1928 −1998	Not computed	30%	9
Wieczorek et al.	2006	Virginia	USA	1	Various species	258	2003	Not computed	Not computed	1
Van Den Eeckhaut et al.	2009	Ardennes	Belgium	1	*Fagus sylvatica*	147	1917 −1998	Not computed	Not computed	25
Lopez saez et al.	2011a	Alps	France	1	*Pinus uncinata*	79	1850 −2008	159	10%	1
Lopez saez et al.	2011b	Alps	France	1	*Pinus uncinata*	403	1900 −2010	704	2%	1
Lopez saez et al.	2012	Alps	France	1	*Pinus uncinata*	223	1900 −2010	355	2%	1
Silhan et al.	2012	Caucasus	Ukraine	1	*Pinus nigra*	48	1702 −2009	150	5%	45
Lopez saez et al.	*in press*	Alps	France	7	*Pinus uncinata*	759	1897 −2010	1298	2%	61

considered the most unstable area in France (Delsigne et al., 2001) and is well known for its extensive mass-movement activity. Extensive records of debris-flow activity exist for the Riou Bourdoux catchment, but conversely, only one landslide event has been inventoried at the study site in spring 1971 (Delsigne et al., 2001).

The Pra Bellon landslide is 175 m long, 450 m wide (32 ha), and has a depth varying between 4 and 9 m. Its elevation ranges from 1470 to 1750 m asl and the volume of the landslide body has been estimated to $1.5–2 \times 10^6$ m^3 (Weber, 1994; Stien, 2001). The rotational landslide is characterized by a 1.5-m-thick top moraine layer underlain by a weathered and unsaturated black marl layer (thickness: 5–6 m), which overlies bedrock of unweathered marl (Mulder, 1991). In dry conditions, black marls are quite solid and able to absorb large quantities of water, but soften considerably when wet. The area is characterized by dry and mountainous Mediterranean climate with strong inter-annual rainfall variability.

According to the HISTALP dataset (Efthymiadis et al., 2006), precipitation at the gridded point closest to the landslide body is 895 ± 154 mm yr^{-1} for the period 1800–2003. Rainfall can be violent, with intensities exceeding 50 mm h^{-1}, especially during frequent summer storms. Melting of the thick snow cover, which forms during the cold months between December and March, only adds to the effect of heavy spring rain (Flageollet, 1999). Mean annual temperature is 7.5 °C with 130 d yr^{-1} of freezing (Maquaire et al., 2003). The study site is characterized by irregular topography with a mean slope angle of ~20°. Mountain pine (*Pinus*

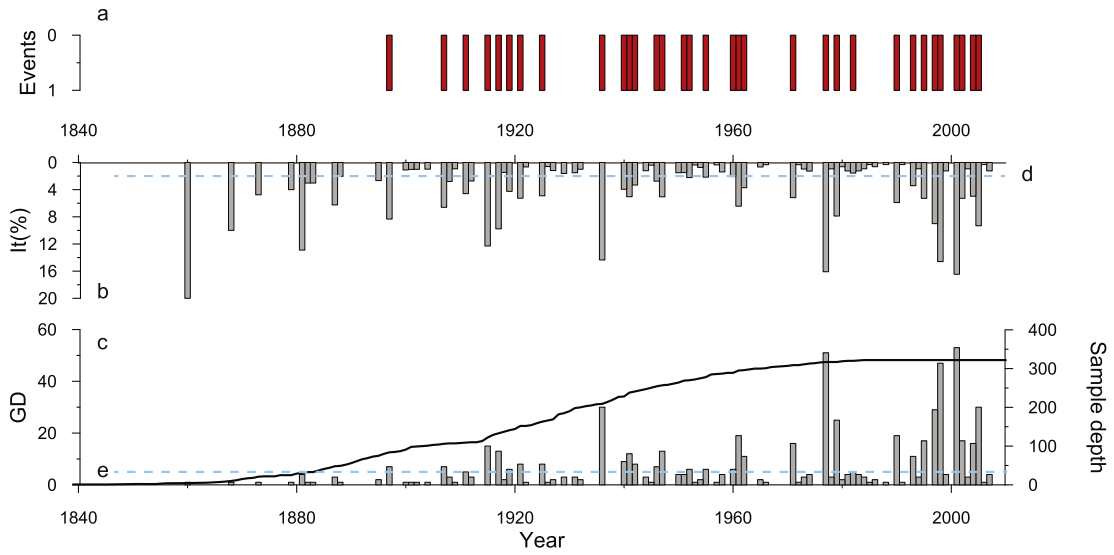

Fig. 2. (a) Event-response histograms with landslide-induced growth disturbances (GD) in sampled trees (b) Percentage of trees and (c) total number of trees responding to a landslide reactivation. Blue horizontal dotted lines demarcate (d) the 2% sample size thresholds, and (e) the $n = 5$ tree number threshold. The black line shows the sample size (i.e. the total number of trees alive in each year). Both empirical thresholds permitted to reconstruct 32 reactivation phases between AD 1897 and 2005. (For interpretation of the references to color in this figure legend, the reader is referred to the web version of this article.)

uncinata) has a competitive advantage on these dry, poor soils (Dehn and Buma, 1999) and forms nearly homogeneous forest stands outside the surfaces affected by the scarps and recent earth slides (Fig. 1b–e).

3. Material and methods

3.1. Reconstruction of landslide reactivation with tree-ring series

Several approaches have been applied in the past to date landsliding with dendrogeomorphic techniques. Tree age may supply first but important hints as to age of the oldest undisturbed tree on a landslide body and may thus provide minimum ages of movement (Carrara and O'Neill, 2003). Pioneering tree-ring work on landslides dates back to McGee (1893) and Fuller (1912). These authors used tree age to establish age and (earthquake) origin of landslides. The original field notes of McGee (1893, p. 413) are remarkable and state that "*along the scarp opposite Reelfoot lake, ancient landslips with their characteristic deformation on the surface are found in numbers. […] Along the sides of the trenches […] trees are frequently thrown out of the perpendicular. These features suggest a sudden and violent movement by which the highly unstable topographic forms of the upland scarp were in part broken down and thrown into more stable positions. […] The great boles two or more centuries old are inclined from root to top, though the younger trees of seventy or seventy-five years usually stand upright, and that the trunks of a century to a century and a half in age are commonly inclined near the ground, but are vertical above.* [Trees thus] *give a trustworthy and fairly accurate date for the production of the minor topographic features a date determined by much counting of annual rings to lie between seventy-five and eighty-five or ninety years ago*".

More recently, landslide reconstructions started to include GD in annual growth-ring series of trees. The first dendrogeomorphic study of a landslide body dates back to Alestalo (1971), and similar field and laboratory approaches have been used ever since in North America (e.g., Shroder, 1978; Reeder, 1979; Hupp, 1983; Osterkamp et al., 1986; Bégin and Filion, 1988; Williams et al., 1992; Carrara and O'Neill, 2003). Table 1 gives an overview on selected tree-ring

Table 2
Minimum, mean and maximum distances between a tree and its three/five nearest neighbors as computed for the best and worst *submaps* derived from sub-samples with sizes varying from 30 to 300 trees.

3 neighbors				5 neighbors			
Sampling	Min distance	Average distance	Max distance	Sampling	Min distance	Average distance	Max distance
Best 30 trees	33.2	94.1	224.1	Best 30 trees	59.5	127.6	230.3
Worst 30 trees	23.3	87.1	187.3	Worst 30 trees	44.7	120.7	216.6
Best 50 trees	29.4	74.1	170.3	Best 50 trees	51.6	101.6	202.6
Worst 50 trees	24.9	70.3	140.3	Worst 50 trees	44.3	94.1	149.8
Best 100 trees	20.2	50.4	136.3	Best 100 trees	25.2	66.3	193.5
Worst 100 trees	12.1	46.7	110.2	Worst 100 trees	24.9	60.8	143.4
Best 150 trees	15.7	36.9	98	Best 150 trees	27.3	50.5	113.3
Worst 150 trees	11.7	35.9	88.5	Worst 150 trees	22.7	41.3	101.5
Best 200 trees	8.4	30.6	103.3	Best 200 trees	13.9	40.5	115.5
Worst 200 trees	8.6	26.9	92.6	Worst 200 trees	12.3	40.3	115.5
Best 250 trees	4.4	25.2	87.7	Best 250 trees	17.1	35.1	89.4
Worst 250 trees	8.4	25.4	89.4	Worst 250 trees	16.2	36.1	105.6
Best 300 trees	4.4	21.5	66.9	Best 300 trees	12.3	31.5	98.6
Worst 300 trees	8.3	22.1	65.7	Worst 300 trees	12.3	32.1	87.8
Validation	4.4	20.5	65.6	Validation	12.3	30.2	87.7

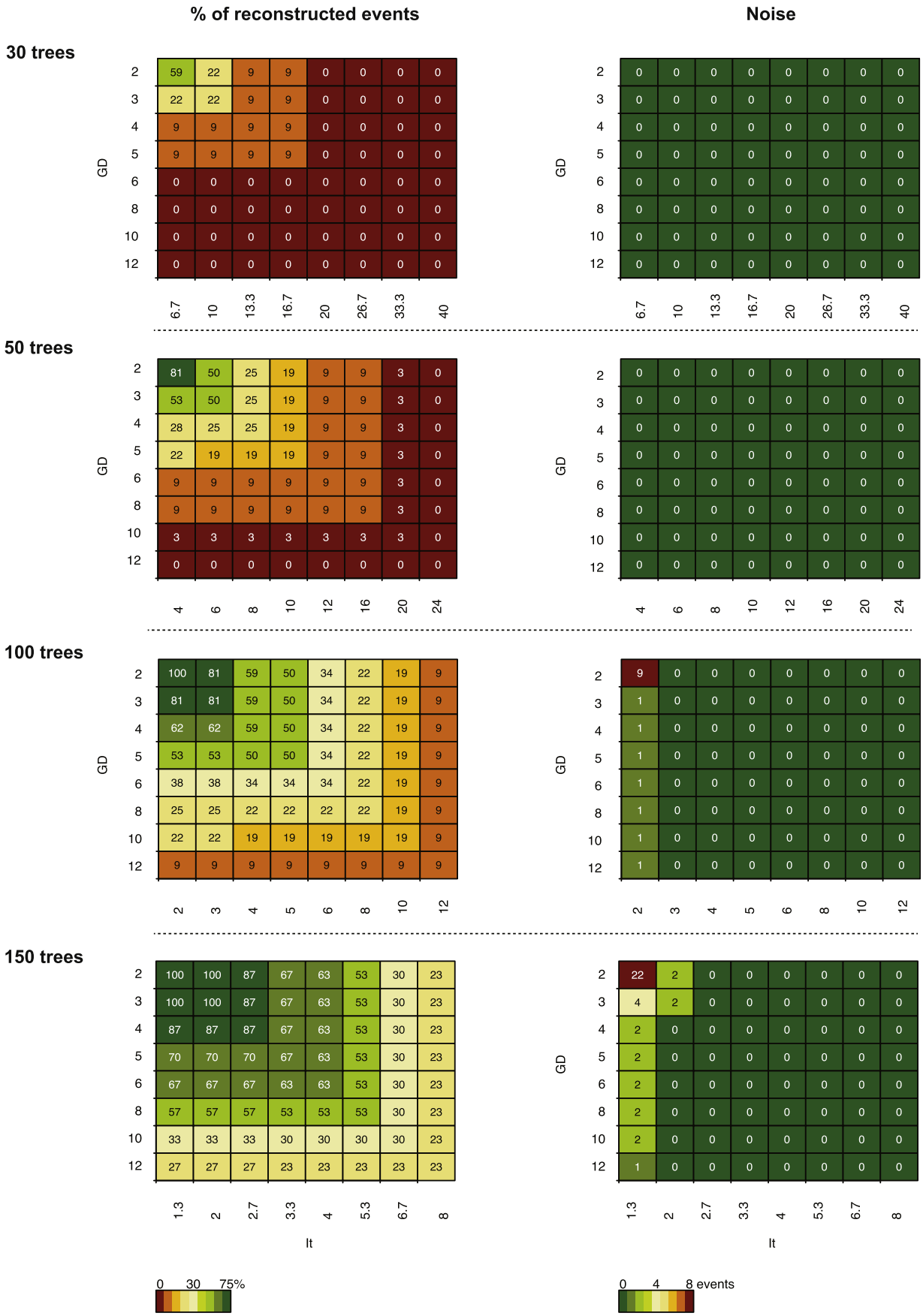

Fig. 3. Percentage of reconstructed events (left panel) and number of additional events (noise; right panel) depending on the number of growth disturbances (GD) and the index value (*It*) used for subsamples varying from 30 to 300 trees.

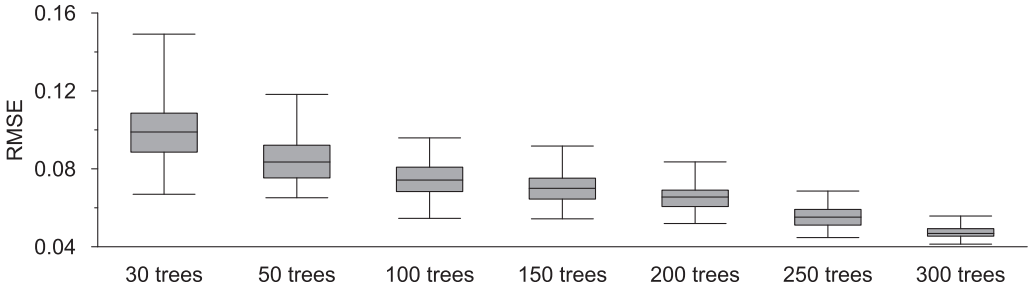

Fig. 4. Boxplots for the Root Mean Square Error (RMSE) between the reference frequency map (Fig. 1e) computed from 323 trees and 100 frequency maps computed with 30–300 randomly extracted trees. Boxplots show minimum, lower quantile (Q 0.25), median (Q 0.5), upper quantile (Q 0.75) and maximum values for each sub-sample.

publications on landslides. In Europe, dendrogeomorphic reconstructions of landslide frequency and reactivations have been introduced much later. They were first used in the French Alps (Braam et al., 1987; Astrade et al., 1998; Lopez Saez et al., 2012a,b) to expand to the Italian Apennines (Fantucci and McCord, 1995; Fantucci and Sorriso-Valvo, 1999), the Spanish Pyrenees (Corominas and Moya, 1999), and more lately to the Belgian Ardennes (Van Den Eeckhaut et al., 2009). Published work does not contain any guidelines on how and how much to sample. As a consequence, past reconstructions of landslide reactivations were based on as little as 13 (Carrara and O'Neill, 2003) to up to as much as 402 trees (Lopez Saez et al., 2011). Similarly, index value (*It*) thresholds (Shroder, 1978) have by far not been used systematically in past work. In case that thresholds were applied, they varied significantly between 2% (Lopez Saez et al., 2012a,b) and 30% (Corominas and Moya, 1999; Stefanini, 2004). Based on the data presented in Table 1, it also becomes obvious that *It* thresholds tend to increase with decreasing sample size and vice versa. In that sense, an *It* >10% would be associated typically with a sample size <60 trees, whereas an *It* ≥ 2% would have been used if the reconstruction was based on a sample size >250 trees.

3.2. Collection and preparation of samples

Based on an outer inspection of the stem, a total of 323 Mountain pines *(Pinus uncinata)* trees (Fig. 1) obviously influenced by past landslide activity were sampled on the Pra Bellon landslide body. Four cores were normally extracted per tree: two in the supposed direction of landslide movement (i.e., upslope and downslope cores) and two perpendicular to the slope. To gather the greatest amount of data on past events, trees were sampled within the tilted segment of the stems.

Trees were processed following standard dendrogeomorphic procedures (Stoffel et al., 2010); individual series were cross-dated using a local reference chronology (Stoffel et al., 2005) to correct the tree-ring records of affected trees for missing or false tree rings. GD in the tree-ring series (i.e. injuries, tangential rows of traumatic resin ducts, compression wood, abrupt growth increase or suppression; see Stoffel and Bollschweiler, 2008 for details) were calendar dated and master chronologies of all GD were then computed for each year and the location of the disturbed trees represented graphically in a Geographic Information System (GIS).

3.3. Testing the optimal sample size and optimal thresholds for landslide reconstructions

With the aim of defining the best sampling design yielding the largest number of past events and a minimum of noise, we first defined years with landslide reactivations using the full dataset of 323 trees (1292 increment cores), archival data from the larger study region, and a classical expert's dendrogeomorphic approach (Schneuwly-Bollschweiler et al., 2013). To account of the larger sample size in more recent years and possible effects thereof on the quantity of GD observed in the tree-ring records, we used the index value (*It*) as defined by Shroder (1978) and Butler and Malanson (1985):

$$It = \left(\sum_{i=1}^{n}(Rt)/\sum_{i=1}^{n}(At)\right)*100 \quad (1)$$

where *R* is the number of trees showing GD as a response to landslide in year *t*, and *A* is the number of sampled trees alive in year *t*. Following disturbance by an initial landslide event, a tree may not necessarily yield useful data on additional events for some time in the sense that it may already be forming a narrow band of annual rings or compression wood such that a subsequent disturbance will not induce an additional reaction and may not thus be detected. This is why *I* was adjusted to only take account of trees with a useful record for year *t* (Carrara and O'Neill, 2003).

Based on the expert chronology, which is considered here as reference, we modeled different sampling designs using sample sizes *(n)* varying from 30 to 300 trees. To reduce the dependence on the sampling itself, and thus to prevent addition of further noise to the reconstruction, 1000 subsets of *n* trees, extracted without replacement, were computed for each sample size *n*. In a subsequent step, GD thresholds from 1 to 10 GD and *It* from 0.3 to 33% were then tested and events added to the reconstruction as soon as both thresholds were exceeded. For each of the modeled sampling designs and thresholds, output was compared with results from the expert chronology to quantify the amount of correctly identified (signal) and misdated (noise) events. Final results are presented in the form of matrices and summarize the mean percentage of reconstructed events documented in the reference chronology and the mean number of events classified as noise according to the *It* and GD thresholds, based on 1000 sampling iterations.

3.4. Testing the optimal sampling strategy and optimal trees for reconstruction

To determine an optimal strategy for future field sampling, an individual frequency of reactivation, expressed as the number of events per year, was computed for each tree as follows:

$$f_T = A_T \div GD_T \quad (2)$$

where *A* represents the total number of years for which tree *T* was alive and where *GD* is the number of growth disturbances related to accepted landslide reactivations in tree *T*. A high-resolution raster frequency map (called *Refmap*) was the produced using an *Inverse Distance Weighting* interpolation of individual frequencies of the 323 *P. uncinata* trees to derive realistic event frequency information

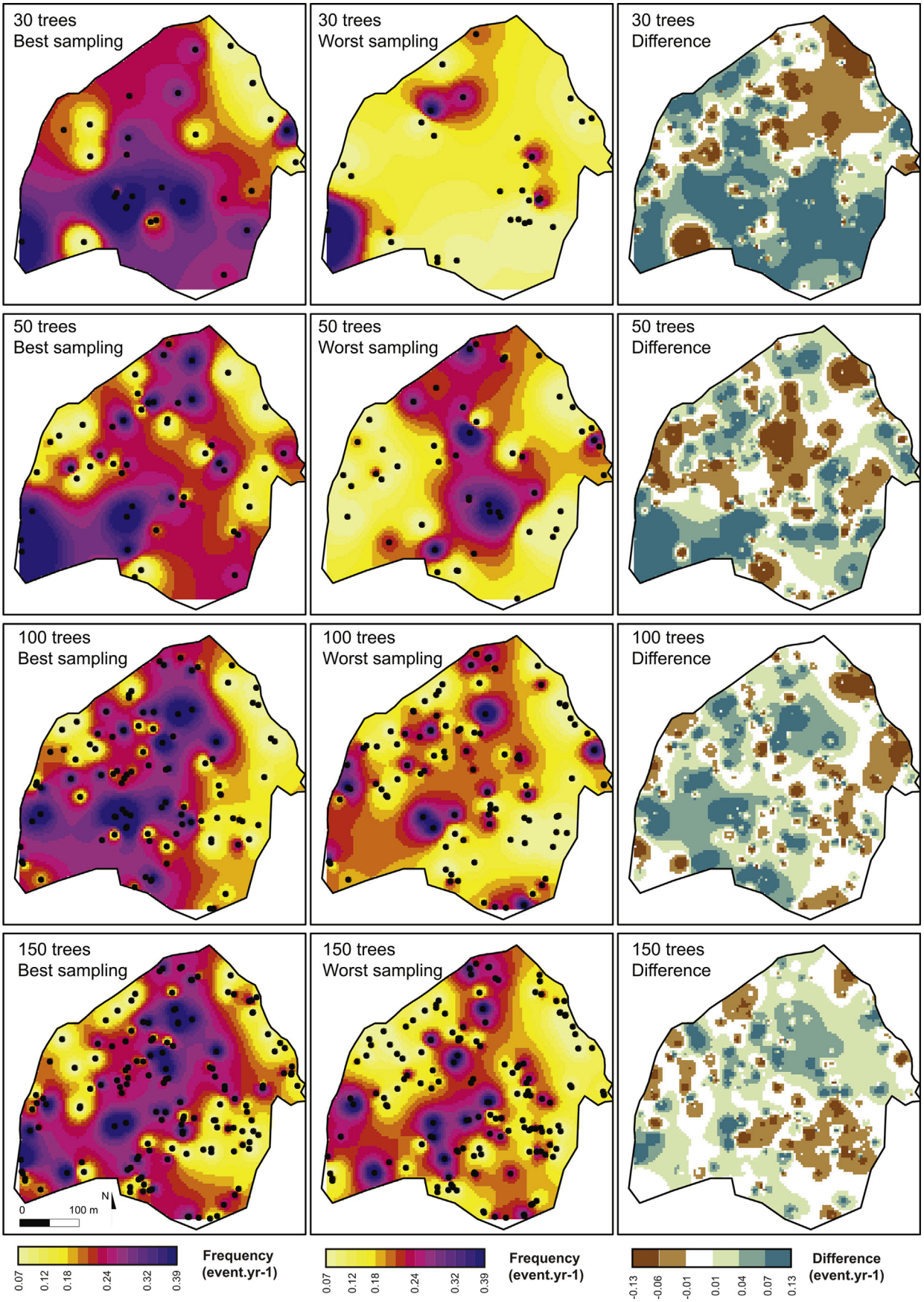

Fig. 5. Best (lowest RMSE, left panel) and worst (highest RMSE, central panel) frequency maps computed from sub-samples of 30–300 randomly extracted trees. Maps on the right panel represent the difference between the best frequency map computed for each sub-sample and the reference map computed with 323 trees (Fig. 1e).

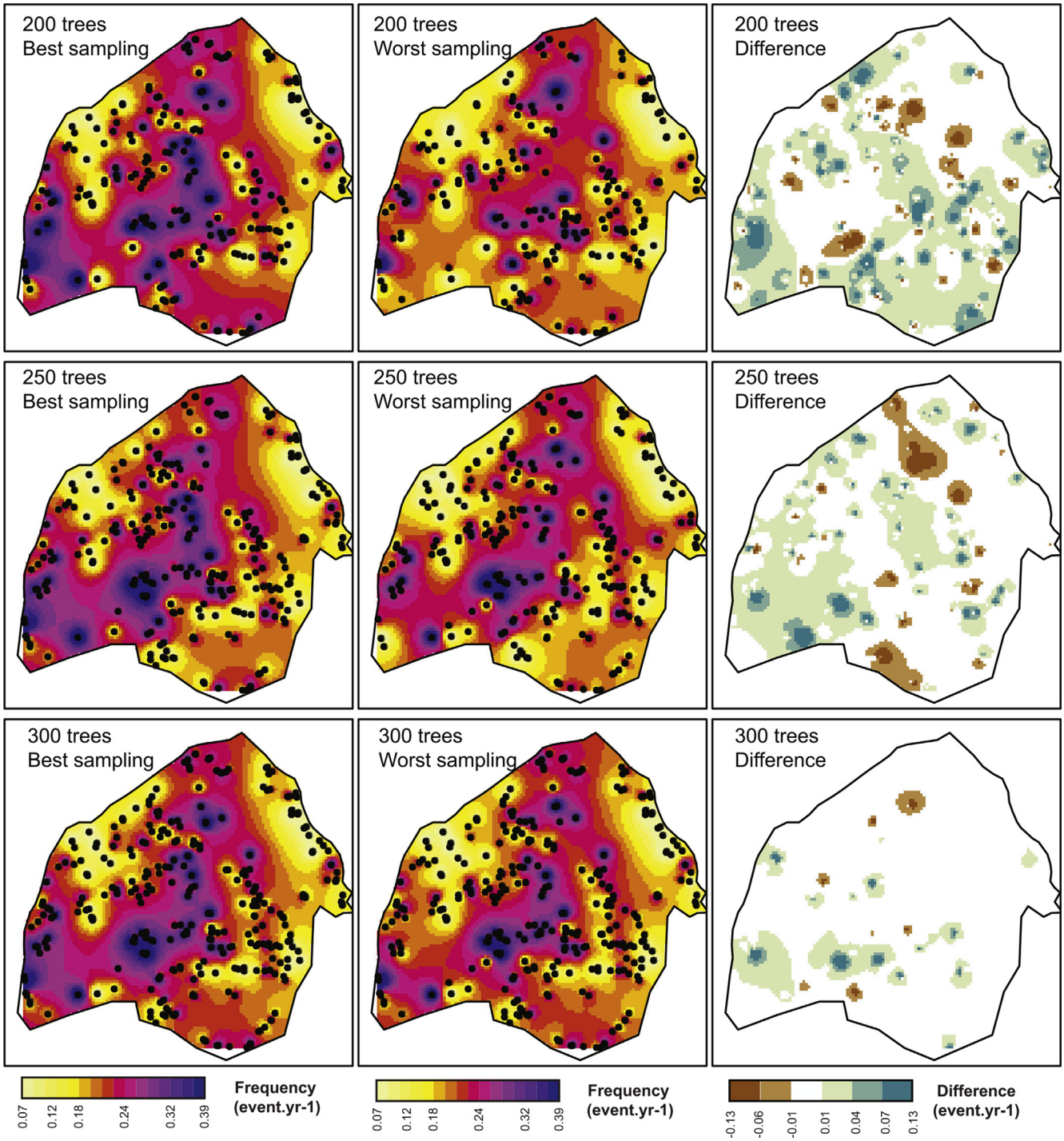

Fig. 5. (*continued*).

for those sectors of the landslide body where dendrogeomorphic techniques could not be used (Fortin and Dale, 2005).

In a subsequent step, 30 to 300 trees were extracted randomly from the original dataset without replacement. This procedure was repeated 100 times. For each subset, we computed (i) a chronology using optimal thresholds (see 3.3) and (ii) individual frequencies of reactivations; and (iii) produced 100 frequency raster maps for each subset. By way of example, a map obtained with a subset of 30 trees was designated *Submap30* in this study and results of individual frequencies were again interpolated using Ordinary Kriging. For each *Submap*, we then (iv) quantified uncertainty in the reconstruction by computing mean Root Mean Square Error (RMSE) from the reference maps *(Refmap)* of the data obtained with the expert's approach as follows:

$$\delta_i = f_{Submap(i)} - f_{Rubmap(i)} \tag{3}$$

$$\text{Mean } RMSE(Submap) = \sqrt{\frac{\sum_{Npix}^{i=1}\left(\delta_1^2 + \delta_2^2 + \cdots + \delta_{Npix}^2\right)}{Npix}} \tag{4}$$

where $f_{submap(i)}$ is the frequency of reactivations interpolated at pixel i in the *Submap*, $f_{refmap(i)}$ represents the frequency of

reactivations interpolated at pixel *i* in the *Refmap*, *Npix* gives the number of pixels in *Refmap* and *Submap* and where δi stands for the discrepancy at pixel *i*.

In a final step, we compared maps with the lowest and the highest RMSE for each of the *Submaps*. For this purpose, the spatial distribution of trees involved in each map was characterized using the ArcGIS spatial statistics tool *"Distance Band from Neighbor Count"* (ESRI, 2011) where the distance of each tree to their nth neighbour is defined with three values: maximum, minimum and average distances, but also contains information on tree age, number of GD and frequency of reactivations. For the purpose of this study, distances were computed for $t = 3$ and $t = 5$, meaning the maximum distance from each tree at which it still has at least *t* neighbors.

4. Results

4.1. Event frequency as reconstructed with the classical expert's approach

Pith ages of the 323 *P. uncinata* trees sampled at Pra Bellon suggest an average age of the stand of 91 ± 28 yr. One-third of the tree sample (32%) is older than 100 yr with the oldest tree selected for analysis showing its first ring at sampling height in AD 1848 (Fig. 2c); the youngest tree reached sampling height in 1983. The distribution of tree ages is heterogeneous and the forest matrix is constituted by trees aged between 50 and 100 yr with patches of old trees (120 yr) scattered within the matrix. According to the tree-ring data, individual old trees were present since the mid-nineteenth century and progressively colonized the landslide body. As a result of the rather dense sampling of *P. uncinata* trees at Pra Bellon landslide body, minimum, mean, and maximum distances between each tree and its three nearest neighbors are 4.4, 20.5 and 65.6 m respectively (Table 2).

A total of 640 GD related to a past landslide event can be identified in the tree-ring record (Fig. 2b). The most common reactions to landslide events are in the form of abrupt growth reductions with 63% of all GD. The onset of compression wood (31%) represents another common response of *P. uncinata* to landsliding. The first GD observed in the tree-ring series dates back to AD 1860.

Based on the empirical threshold fixed at GD ≥ 5 and It >2% (Figs. 2b, c), 32 landslide reactivation phases could be dated for the period 1897–2005, namely in 1897, 1907, 1911, 1915, 1917, 1919, 1921, 1925, 1936, 1940, 1941, 1942, 1946, 1947, 1952, 1955, 1960, 1961, 1962, 1971, 1977, 1979, 1982, 1989, 1993, 1995, 1997, 1998, 2001, 2002, 2004, and 2005 (Fig. 2a), representing a frequency of reactivations for the Pra Bellon landslide of 0.3 events yr^{-1}. If analyzed spatially, the frequency shows a clear decrease from the central part (0.39 event yr^{-1}) to the margins (0.07 event yr^{-1}) of the landslide body (Fig. 1e). Due to lacking independent archival records from the landslide body itself and the fact that the tree-ring record retrieved from Pra Bellon is clearly the largest so far, the chronology and frequency maps obtained with the expert's approach were considered as a reference for the subsequent testing of thresholds and sampling design.

4.2. Defining optimal GD and It thresholds with differing sample sizes

Using the time series of landslide reactivations obtained with the expert's approach, we modeled various sample sizes (*n*) varying from 30 to 300 trees to observe differences in the number of reconstructed events and in optimal GD and *It* thresholds. Fig. 3 shows results of subsets of 30 (Fig. 3a), 50 (Fig. 3b), and 100 trees (Fig. 3c), for which 59% (GD ≥ 2, It ≥ 6.7%), 81% (GD ≥ 2, *It* ≥ 4%), and 81% (GD ≥ 3, It ≥ 3%), respectively, of the signls – in terms of landslide events listed in the expert chronology – could be reconstructed without including noise in the time series. Fig. 3d illustrates that a subset of 150 trees and a GD ≥ 4, and *It* ≥ 2.7% would allow for 87% of all events to be reconstructed correctly. The ratio of signal-to-noise does not increase significantly with a sample size of 200 trees (Fig. 3e). By contrast, all events identified in the expert's approach can be reconstructed correctly with a minimal number of 250 trees and thresholds set at GD ≥ 5 and *It*≥1.6% (Fig. 3f). A sample size of 50–100 trees can thus be considered a good compromise between field efforts, laboratory analyses and the results obtained.

4.3. Determining an optimal sampling design

Based on the above considerations on sample size, GD and *It* thresholds, we aimed at defining the best sampling design which yields optimal spatial information with a minimum of noise. We again modeled different sampling designs with different sample sizes and extracted 100 subsets of *n* trees (*n* varying between 30 and 300) for each sample size to reduce dependence of results on sampling location. Fig. 4 illustrates differences between the reference frequency map (*Refmap*), computed with all sampled trees, and the best (i.e. min. *mean RMSE*) and worst (i.e. max. *mean RMSE*) *Submaps* obtained for the different subsets. Not surprisingly, *mean RMSE (Submap)* decrease by >50% with increasing sample size, and vary between 0.09 ± 0.09 event yr^{-1} for *Submap30* to 0.04 ± 0.002 event yr^{-1} for *Submap300*. Noteworthy, the best *Submap50* has an RMSE comparable to the average RMSE obtained for *Submap200*. Moreover, significant discrepancies exist between the worst and the best *Submaps* for a given sample size (Fig. 5d), thereby pointing to clear dependancies between mean RMSE and sampling design, i.e. the spatial distribution of trees selected for the interpolation, especially for subsets <200 trees.

In an attempt to tackle the issue of sampling design further and to relate the impact of the spatial distribution of sampled trees on the quality (i.e. best and worst) of *Submaps*, we used the ArcGIS spatial statistics «*Distance Band from Neighbor Count*» tool. Table 2 illustrates that the best interpolation based on 30 trees (*Submap*30) is obtained when the minimum, mean, and maximum distances between a tree and its three nearest neighbours are 33, 94, and 224 m, respectively. A comparison with the worst *Submap30* shows significantly lower values (i.e. 23, 87, and 187 m), thereby pointing to a clustering of trees selected. Differences between the best and worst *Submaps* remain comparable if five neighbors are taken into account. Higher distances between trees are obtained systematically for the best as compared to the worst *Submaps* for all sample sizes <200 trees.

4.4. Selecting «optimal» trees for landslide mapping

Interestingly, the mean RMSE is not correlated significantly to tree age, and this independently of sample size taken into account in the subsample ($R^2 = 0.0007$ to 0.06 for subsets of 200 and 50 trees, respectively; Fig. 6). The best and worst *Submap150, Submap200,* and *Submap300*, for instance, were derived from trees with comparable mean ages (Fig. 7). Conversely, the best *Submap30* and *Submap50* are derived from slightly older trees (mean age 95.6 and 94.6 yr, respectively) than the worst *Submap30* and *Submap50* (mean age 92.9 yr) whereas the best *Submap100* is obtained with slightly younger trees (89.7 yr) than the worst *Submap100* (93 yr).

By contrast, significant negative correlations ($p < 0.001$) are obtained between mean RMSE and mean number of GD observed in trees for all subsets (Fig. 6). In other words, the precision of the frequency maps will always increase if sampling is based on

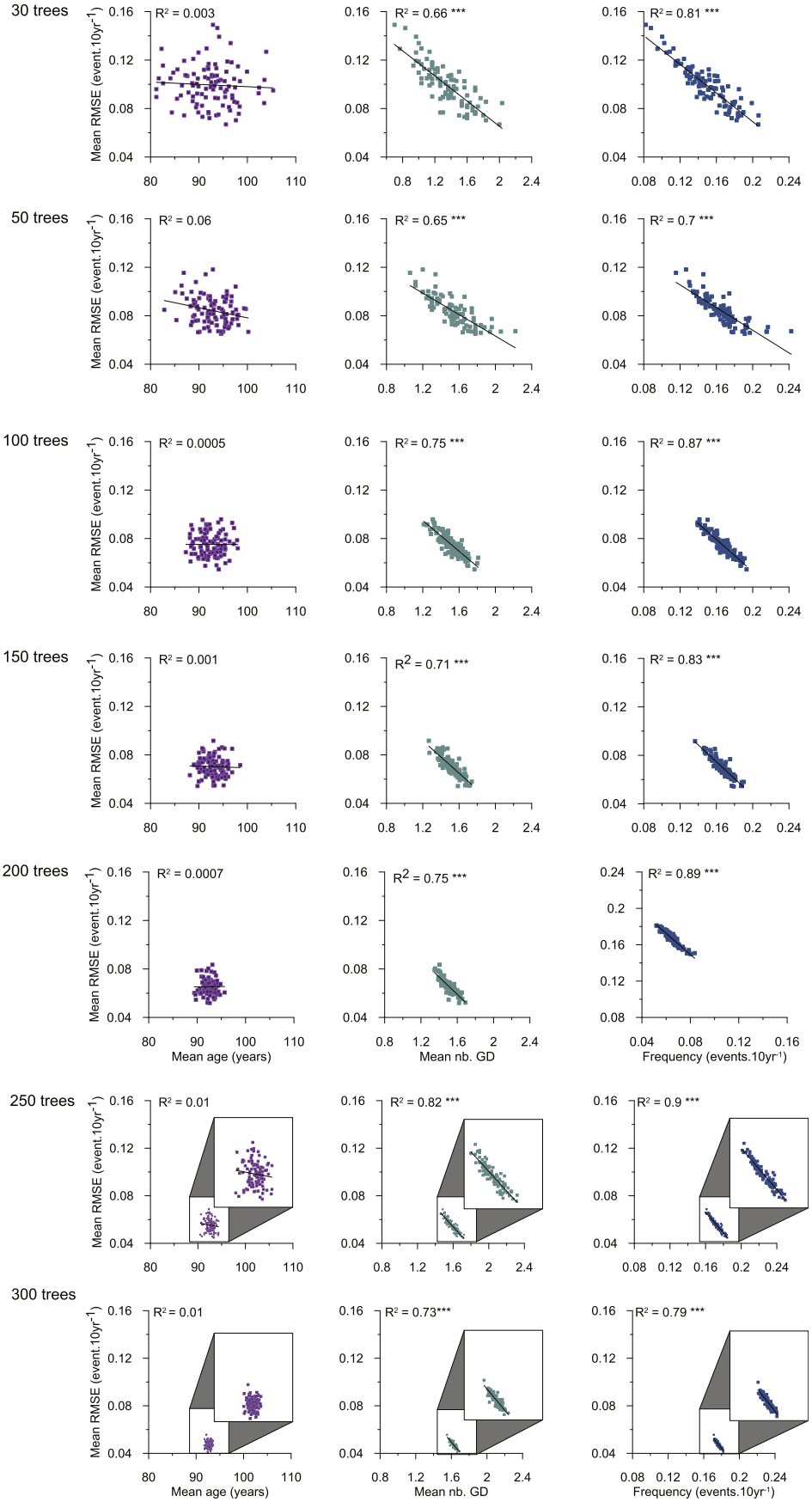

Fig. 6. Correlations between RMSE and tree age (left panel), number of GD (central panel) and the mean frequency of GD per tree (right panel) computed for each of the 100 sub-samples with sample sizes varying from 30 to 300 trees. For each graph, the coefficient of determination and the significance of the regression (p-value) are given. Blanks are not statistically significant, $p < 0.1$, $^{*}p < 0.05$, $^{**}p < 0.01$, $^{***}p < 0.001$.

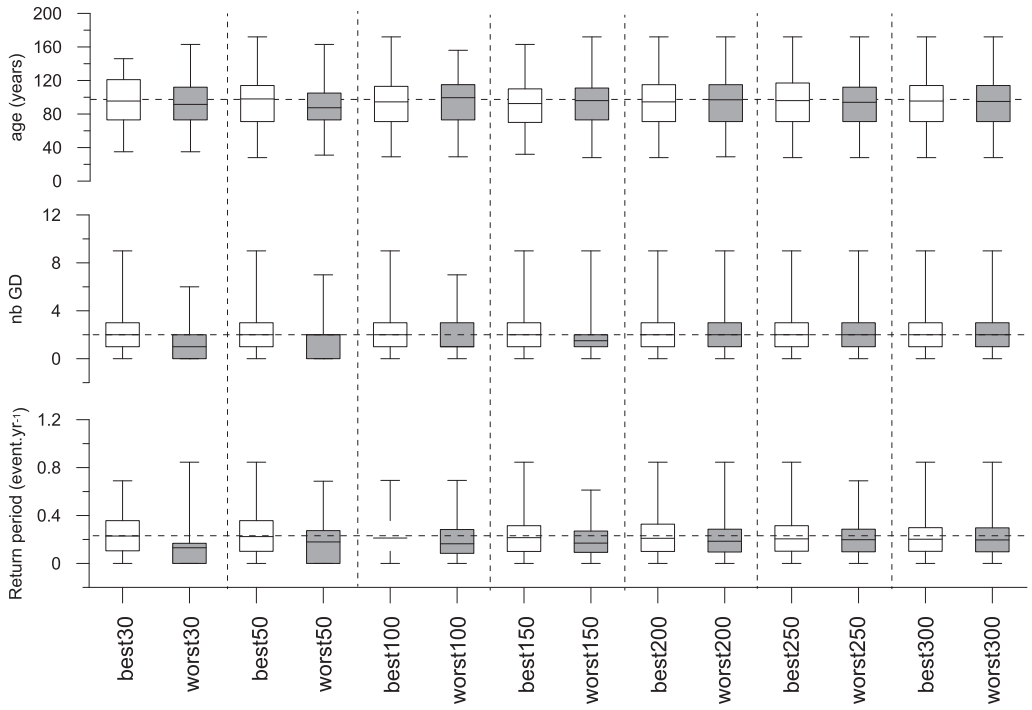

Fig. 7. Boxplot for tree age (top), number of GD (centre) and mean frequency (bottom) of GD per tree computed for the best and worst frequency *submaps* derived from sub-samples with sizes varying from 30 to 300 trees.

frequently damaged trees. Highly significant correlations ($p < 0.001$) can also be observed between mean RMSE and mean GD frequency at the tree level with coefficients of determination ranging from 0.79 to 0.89. The slope of the regression lines indicates a decrease of the mean RMSE of 0.02 if the mean GD frequency at the tree level decreases by 0.4 event yr^{-1}.

5. Discussion

5.1. Optimal sample size for the temporal reconstruction

In his seminal paper, Shroder (1978) emphasized that sample size may be a moot question unless site selection ensures that trees are responding to the process under investigation. Site selection is for sure important (Stoffel and Bollschweiler, 2008), but consider that Butler's et al. (1987) questions of how many trees should be sampled and how many of the sampled trees must illustrate tree-ring responses for an event to be inferred should be seen as at least equally critical.

As the sample size used in this study exceeds that of most other published work in a quite substantial matter (Table 1), we attempted to address the definition of optimal index values and the influence of sample size, spatial sample design as well as GD and *It* thresholds on the reconstructed time series. For this purpose, we used various subsets of an existing landslide chronology (323 trees) and modeled sample sizes varying from 30 to 300 trees. Results demonstrate very clearly that the number of landslide reactivations replicated with tree-ring records depends on sample size up to an optimum of ~250 disturbed trees, and that results remain relatively stable above this value. Interestingly, we also realize that a sample size of ~50 trees might be enough to capture 81%. The missed events (19%) were characterized by smaller *It* in the expert's reconstruction and could thus be the result of minor reactivations.

The optimal sample size obtained for landslides is slightly lower than the values previously suggested for tree-ring based snow avalanche and debris-flow reconstructions, where ~100 (Corona et al., 2012) and ~150 trees (Schneuwly-Bollschweiler et al., 2013), respectively, have been proposed as an appropriate minimum sample size for reasonable reconstructions with limited or no noise. In contrast to snow avalanches and debris flows, landslides will tend to spread considerably and likely leave larger spatial footprints, and will thus be recorded by a larger number of trees (Perret et al., 2006). Based on the results of the bootstrap random extraction, we also realize that GD and *It* thresholds should be defined in a flexible way and that these values will need to be adapted depending on the number of trees available for analysis at different periods of the past (Corona et al., 2012; Stoffel et al., 2013). For example, when sample size is 200 trees, a 1% It infers a landslide event on the basis of two GD and therefore induces a lot of noise (30 undocumented events) into the reconstruction. On the other extreme, an It threshold of 5% appears to be much too stringent and only 53% of the events reconstructed based on the expert approach reconstruction would have been recognized in the tree-ring series. Based on these considerations and on the results presented in Fig. 3, our study suggests that an optimal index value of ~5% (GD $\geq$ 2) should be used with a small sample size (30–50 trees) to capture a maximum of landslide event without introducing noise. With a larger sample size (>200 trees), the optimal It can be reduced to 2.5% (GD $\geq$ 5) without introducing significant noise to the reconstruction.

5.2. Optimal sampling design for spatial reconstructions of landslides and interpolations

The next critical issue addressed in this paper was the design of sampling in the field, i.e. the definition of where trees are sampled on the object under study. Various sampling strategies have been used in the literature to derive interpolations of return periods derived from tree-ring records. In a majority of landslide sites and in the case of most dendrogeomorphic work focusing on other

mass-wasting processes, trees were selected randomly and the selection of trees was dictated by the occurrence of visible growth defects on stems. Sampling in this case was realized with detailed geomorphic maps, a visual inspection of the stem and based on expert opinions (Lopez Saez et al., 2012a,b). On rockfall sites, on the other hand, sampling was realized more systematically and organized along vertical and/or horizontal transects (Moya et al., 2010). Stoffel et al. (2005) or Schneuwly and Stoffel (2008a), for example, developed a sampling design where trees were sampled every *n* meters along horizontal profiles (or transects) to ensure an even distribution of sampled trees. Among the trees located at the place *t* be sampled, however, the most heavily affected tree was sampled preferentially. Moya et al. (2010), on the other hand, performed an exhaustive sampling of all visible tree injuries in 15–30-m wide horizontal forest strips located parallel to the contour lines so as to detect all rockfall trajectories. On avalanche paths, Muntan et al. (2009) adopted a composite sampling design and sampled trees along transects (systematic sampling), but also included all trees located outside transects but showing growth defects related to past avalanches (random sampling). In the case of torrential (i.e. debris floods, debris flows, or lahars), Schneuwly-Bollschweiler et al. (2013) tested varying sampling sizes at specific radial distances from the fan apex and increasing lateral distance from the channel, and demonstrated that maximizing sample size near the cone apex – where avulsion is more likely to occur – would provide better results than would trees cored along the debris-flow channel.

The approach presented in this paper determines the best sampling design using bootstrap random sampling and iterative (interpolation) mapping techniques. We confirm that best frequency maps are obtained with the largest sample sizes. More interestingly, however, we demonstrate that (i) important discrepancies exist between the best and the worst frequency *submaps* for sample sizes <200 trees. As most published work on landslide activity was realized with far less than 200 trees (see Table 1), one might question the completeness and accuracy of these studies as far as the temporal frequency of reactivations and the spatial coherency of interpolated return periods is concerned. Based on bootstrap random extractions, we also illustrate that (ii) the spatial distribution of trees will influence the quality of frequency maps quite clearly, and that the lowest RMSE are obtained if trees are (iii) evenly distributed on the landslide body, (iv) clustered sampling is avoided in those areas with frequent reactivations and if (v) frequently damaged trees are sampled preferentially.

Interestingly, our analysis also revealed that the smallest RMSE obtained with the best constellation of 50 trees (i.e. *submap50*) was comparable to the mean RMSE of *submap200*, meaning that 50 trees collected at the right locations would yield as good results as 200 trees selected randomly on the landslide body. We can thus suggest to limit sample size in future work, provided that priority is given to stratified sampling where the most heavily affected trees are sampled with a homogenous pattern over the entire study area.

6. Conclusion

Evaluating the potential of tree-ring analysis on an extensively sampled landslide in the Ubaye valley (southern French Alps) reveals that as little as 50–100 trees can be sufficient to obtain a reasonably good match between reconstructions and archives (or expert approaches in the present case) while minimizing the inclusion of noise in the dendrogeomorphic record. This sample size should not be seen as a rigid threshold and will always need to be adapted to local conditions, but nevertheless confirm the assumption that event chronologies of processes with a large spread, such as landslides, will leave larger spatial footprints (Perret et al., 2006) and could thus be sampled with smaller sample sizes than discrete processes. We also conclude that GD thresholds need to be adjusted to sample size and should be preferred over fixed values. In addition, an even distribution of samples across the study site and the selection of the most impacted trees are yet other prerequisites to increase reliability of interpolated frequency (or return period) maps in case that reconstructions are based on small sample sizes. An optimized minimum sample size and an appropriate sampling design will ultimately facilitate fieldwork, and thus render analyses and interpretation more reliable, less time consuming and improve cost-benefit ratios. Based on the sample sized defined in this study, we indeed believe that dendrogeomorphic techniques clearly represent a complimentary but competitive data source on past disasters and that it should be included more frequently in conventional risk assessments at exposed sites covered by forest.

Definition of the sample size, sampling design as well as GD and *It* values presented in this paper was based on the idea of cost-benefit ratios where a minimization of field efforts and a maximization of reconstructed events without noise was challenged. At the same time, however, we are fully aware that fundamental research will not so much be guided by temporal constraints but rely on larger sample sizes in the future as well, especially if it focuses the validation and/or calibration of physically-based mass-movement models (Stoffel et al., 2006; Ballesteros et al., 2011a, b; Corona et al., 2013), the assessment of mass-movement triggers (Schneuwly and Stoffel, 2008; Silhan, 2012) or the analysis of climate – mass-movement interactions (Lugon and Stoffel, 2010; Stoffel et al., 2011; Schneuwly-Bollschweiler and Stoffel, 2012).

Editorial handling by: F. Preusser

Appendix A. Supplementary data

Supplementary data related to this article can be found at http://dx.doi.org/10.1016/j.quageo.2014.02.006.

References

Alestalo, J., 1971. Dendrochronological interpretation of geomorphic processes. Fennia 105, 1–139.
Astrade, L., Bravard, J., Landon, N., 1998. Mouvements de masse et dynamique d'un géosysteme alpestre: etude dendrogeomorphologique de deux sites de la vallée de Boulc (Diois, France). Géogr. Phys. Quat. 52, 153–166.
Baillie, M.G.L., 2008. Proposed re-dating of the European ice core chronology by seven years prior to the 7th century AD. Geophys. Res. Lett. 35, L15813.
Ballesteros, J.A., Bodoque, J.M., Díez-Herrero, A., Sanchez-Silva, M., Stoffel, M., 2011a. Calibration of floodplain roughness and estimation of flood discharge based on tree-ring evidence and hydraulic modelling. J. Hydrol. 403, 103–115.
Ballesteros, J.A., Eguibar, M., Bodoque, J.M., Díez-Herrero, A., Stoffel, M., Gutiérrez-Pérez, I., 2011b. Estimating flash flood discharge in an ungauged mountain catchment with 2D hydraulic models and dendrogeomorphic palaeostage indicators. Hydrol. Process. 25, 970–979.
Bégin, C., Filion, L., 1988. Age of landslides along the grande rivière de la Baleine estuary, Eastern coast of Hudson bay, Québec (Canada). Boreas 17, 289–299.
Bekker, M.F., 2010. Tree rings and earthquakes. In: Stoffel, M., Bollschweiler, M., Butler, D.R., Luckman, B.H. (Eds.), Tree Rings and Natural Hazards: a State-of-the-art. Springer, Heidelberg, New York, pp. 391–397.
Bollschweiler, M., Stoffel, M., Vazquez Selem, L., Palacios, D., 2009. Tree-ring reconstruction of past lahar activity at Popocatepetl volcano, Mexico. Holocene 20, 265–274.
Braam, R., Weiss, E., Burrough, P., 1987. Spatial and temporal analysis of mass movement using dendrochronology. Catena 14, 573–584.
Butler, D.R., Malanson, G.P., 1985. A reconstruction of snow-avalanche characteristics in Montana, USA, using vegetation indicators. J. Glaciol. 31 (108), 185e187.
Butler, D.R., Malanson, G., Oelfke, J., 1987. Tree-ring analysis and natural hazard chronologies: minimum sample sizes and index values. Prof. Geogr. 39, 41–47.
Butler, D.R., Sawyer, C.F., 2008. Dendrogeomorphology and high-magnitude snow avalanches: a review and case study. Nat. Hazards Earth Syst. Sci. 8 (2), 303e309.
Carrara, P., O'Neill, J.M., 2003. Tree-ring dated landslide movements and their relationship to seismic events in southwestern Montana, USA. Quat. Res. 59, 25–35.

Corominas, J., Moya, J., 1999. Reconstructing recent landslide activity in relation to rainfall in the Llobregat River basin, eastern Pyrenees, Spain. Geomorphology 30, 79–93.
Corona, C., Rovéra, G., Lopez Saez, J., Stoffel, M., Perfettini, P., 2010. Spatio-temporal reconstruction of snow avalanche activity using tree rings: Pierres Jean Jeanne avalanche talus, Massif de l'Oisans, France. Catena 83, 107–118.
Corona, C., Saez, J.L., Stoffel, M., Bonnefoy, M., Richard, D., Astrade, L., Berger, F., 2012. How much of the real avalanche activity can be captured with tree rings? An evaluation of classic dendrogeomorphic approaches and com-parison with historical archives. Cold Regions Sci. Technol. 74-75, 31e42.
Corona, C., Trappmann, D., Stoffel, M., 2013. Parameterization of rockfall source areas and magnitudes with ecological recorders - when disturbances in trees serve the calibration and validation of simulation runs. Geomorphology 202, 33–42. http://dx.doi.org/10.1016/j.geomorph.2013.02.001.
Dehn, M., Buma, J., 1999. Modelling future landslide activity based on general circulation models. Geomorphology 30, 175–187.
Delsigne, F., Lahousse, P., Flez, C., Guiter, G., 2001. Le Riou Bourdoux: un "monstre" alpin sous haute surveillance. Rev. For. Française, 527–541.
Efthymiadis, D., Jones, P.D., Briffa, K.R., Auer, I., Böhm, R., Schöner, W., Frei, C., Schmidli, J., 2006. Construction of a 10-min-gridded precipitation data set for the greater alpine region for 1800–2003. J. Geophys. Res. http://dx.doi.org/10.1029/2005JD006120.
ESRI, 2011. ArcGIS 10.1 (Redlands, CA).
Fantucci, R., McCord, A., 1995. Reconstruction of landslide dynamic with dendrochronological methods. Dendrochronologia 13, 43–58.
Fantucci, R., Sorriso-Valvo, M., 1999. Dendrogeomorphological analysis of a slope near Lago, Calabria (Italy). Geomorphology 30, 165–174.
Flageollet, J., 1999. Landslides and climatic conditions in the Barcelonnette and Vars basins (southern French Alps, France). Geomorphology 30, 65–78.
Fortin, M.-J., Dale, M.R.T., 2005. Spatial Analysis. A Guide for Ecologists. Cambridge University Press, Cambridge.
Fuller, M., 1912. The New Madrid Earthquake. Center for Earthquake Studies, Southeast Missouri State University, Cape Girardeau.
Hupp, C.R., 1983. Geo-botanical evidence of late Quaternary mass wasting in block field areas of Virginia. Earth Surf. Process. Landforms 8, 439–450.
Jacoby, G.C., Sheppard, P.R., Sieh, K.E., 1988. Irregular recurrence of large earthquakes along the San Andreas fault: evidence from trees. Science 241, 196–199.
Lopez Saez, J., Corona, C., Stoffel, M., Berger, F., 2011. Probability maps of landslide reactivation derived from tree-ring records: Pra Bellon landslide, Southern French Alps. Geomorphology 138, 189–202.
Lopez Saez, J., Corona, C., Stoffel, M., Astrade, L., Berger, F., Malet, J.-P., 2012a. Dendrogeomorphic reconstruction of past landslide reactivation with seasonal precision: the Bois Noir landslide, southeast French Alps. Landslides 9, 189–203.
Lopez Saez, J., Corona, C., Stoffel, M., Berger, F., 2012b. High-resolution fingerprints of past landsliding and spatially explicit, probabilistic assessment of future reactivations: Aiguettes landslide, southeastern French Alps. Tectonophysics 602, 355–369. http://dx.doi.org/10.1016/j.tecto.2012.04.020.
Lopez Saez, J., Corona, C., Stoffel, M., Berger, F., 2013. Climate change increases the frequency of snowmelt-induced landslides in the French Alps. Geology 41 (5), 619–622. http://dx.doi.org/10.1130/G34098.1.
Lugon, R., Stoffel, M., 2010. Rock-glacier dynamics and magnitude–frequency relations of debris flows in a high-elevation watershed: Ritigraben, Swiss Alps. Global Planet. Change 73, 202–210.
Maquaire, O., Malet, J.P., Remaître, A., Locat, J., Klotz, S., Guillon, J., 2003. Instability conditions of marly hillslopes: towards landsliding or gullying? The case of the Barcelonnette basin, south east France. Eng. Geol. 70, 109–130.
McAuliffe, J.R., Scuderi, L.A., McFadden, L.D., 2006. Tree-ring record of hillslope erosion and valley floor dynamics: landscape responses to climate variation during the last 400 yr in the Colorado Plateau, northeastern Arizona. Global Planet. Change 50, 184–201.
McGee, W.J., 1893. A fossil earthquake. Geol. Soc. Am. Bull. 4, 411–414.
Moya, J., Corominas, J., Perez-arcas, J., Baeza, C., 2010. Tree-ring based assessment of rockfall frequency on talus slopes at Solà d'Andorra, Eastern Pyrenees. Geomorphology 118, 393–408.
Mulder, H., 1991. Assessment of Landslide Hazard. Ph.D. thesis. Faculty of Geographical Sciences, University of Utrecht, Netherlands, p. 149.
Muntan, E., Garcia, C., Oller, P., Marti, G., Garcia, A., Gutierrez, E., 2009. Reconstructing snow avalanches in the Southeastern Pyrenees. Nat. Hazards Earth Syst. Sci. 9, 1599–1612.
Osterkamp, W., Hupp, C., Blodgett, J., 1986. Magnitude and Frequency of Debris Flows, and Areas of Hazard on Mount Shasta, p. 21. California. Geological Survey Professional Paper 1396-C, Vancouver, WA.
Osterkamp, W.R., Hupp, C.R., Stoffel, M., 2012. The interactions between vegetation and erosion: new directions for research at the interface of ecology and geomorphology. Earth Surf. Process. Landforms 37, 23–36.
Perret, S., Stoffel, M., Kienholz, H., 2006. Spatial and temporal rockfall activity in a forest stand in the Swiss Prealps – a dendrogeomorphological case study. Geomorphology 74 (1–4), 219–231.
Reeder, J., 1979. The dating of landslides in Anchorage, Alaska. A case for earthquake trig-gered movements. Geol. Soc. Am. Abstr. Programs, 501.
Salzer, M.W., Hughes, M.K., 2007. Bristlecone pine tree rings and volcanic eruptions over the last 5000 yr. Quat. Res. 67, 57–68.
Schläppy, R., Jomelli, V., Grancher, D., Stoffel, M., Corona, C., Brunstein, D., Eckert, N., Deschatres, M., 2013. The crucial role of the expertise in the determination of snow avalanche based on tree-ring records – a statistical validation of the consistency and transferability of a semi-quantitative approach. Arct. Antarct. Alp. Res. 45, 383–393.
Schneuwly, D.M., Stoffel, M., 2008. Tree-ring based reconstruction of the seasonal timing, major events and origin of rockfall on a case-study slope in the Swiss Alps. Nat. Hazards Earth Syst. Sci. 8 (2), 203–211.
Schneuwly-Bollschweiler, M., Stoffel, M., 2012. Hydrometeorological triggers of periglacial debris flows – a reconstruction dating back to 1864. J. Geophys. Res. – Earth Surf. 117, F02033.
Schneuwly-Bollschweiler, M., Corona, C., Stoffel, M., 2013. How to improve dating quality and reduce noise in tree-ring based debris-flow reconstructions. Quat. Geochronol. 18, 110–118. http://dx.doi.org/10.1016/j.quageo.2013.05.001.
Shroder, J.F., 1978. Dendrogeomorphological analysis of mass movement on table Cliffs Plateau, Utah. Quat. Res. 9 (2), 168e185.
Silhan, K., 2012. Dendrogeomorphological analysis of the evolution of slope processes on Flysch rocks (Vsetinske Vrchy Mts, Czech Republic). Carpathian J. Earth Environ. Sci. 7, 39–49.
Stahle, D.W., Fye, F.K., Therrel, M.D., 2003. Interannual to decadal climate and streamflow variability estimated from tree rings. In: van der Meer, J. (Ed.), Developments in Quaternary Sciences, 1. Elsevier, Amsterdam, pp. 491–504.
Stefanini, M., 2004. Spatio-temporal analysis of a complex landslide in the Northern Apennines (Italy) by means of dendrochronology. Geomorphology 63, 191–202.
St George, S., Nielsen, E., 2002. Hydroclimatic change in southern Manitoba since A.D. inferred from tree rings. Quat. Res. 58, 103–111.
Stien, D., 2001. Glissements de terrains et enjeux dans la vallée de l'Ubaye et le pays de Seyne. Rapport RTM, Barcelonnette, France, p. 218.
Stoffel, M., Schneuwly, D., Bollschweiler, M., Lièvre, I., Delaloye, R., Myint, M., Monbaron, M., 2005. Analyzing rockfall activity (1600–2002) in a protection forest – a case study using dendrogeomorphology. Geomorphology 68, 224–241.
Stoffel, M., Wehrli, A., Kühne, R., Dorren, L.K.A., Perret, S., Kienholz, H., 2006. Assessing the protective effect of mountain forests against rockfall using a 3D simulation model. For. Ecol. Manag. 225, 113–122.
Stoffel, M., Bollschweiler, M., 2008. Tree-ring analysis in natural hazards research – an overview. Nat. Hazards Earth Syst. Sci. 8, 187–202.
Stoffel, M., Conus, D., Grichting, M.A., Lièvre, I., Maître, G., 2008. Unraveling the patterns of late Holocene debris-flow activity on a cone in the Swiss Alps: chronology, environment and implications for the future. Global Planet. Change 60, 222–234.
Stoffel, M., Bollschweiler, M., Butler, D.R., Luckman, B., 2010. Tree Rings and Natural Hazards. Springer, Dordrecht; New York.
Stoffel, M., Bollschweiler, M., Vazquez-Selem, L., Franco-Ramos, O., Palacios, D., 2011. Dendrogeomorphic dating of rockfalls on low-latitude, high-elevation slopes: Rodadero, Iztaccíhuatl volcano, Mexico. Earth Surf. Process. Landforms 36, 1209–1217.
Stoffel, M., Wilford, D.J., 2012. Hydrogeomorphic processes and vegetation: disturbance, process histories, dependencies and interactions. Earth Surf. Process. Landforms 37, 9–22.
Stoffel, M., Butler, D.R., Corona, C., 2013. Mass movements and tree rings: a guide to dendrogeomorphic field sampling and dating. Geomorphology 200, 106–120. http://dx.doi.org/10.1016/j.geomorph.2012.12.01.
Stoffel, M., Corona, C., 2014. Dendroecological dating of geomorphic disturbance in trees. Tree Ring Res 70, 3–2.
Trappmann, D., Stoffel, M., 2013. Counting scars on tree stems to assess rockfall hazards: a low effort approach, but how reliable? Geomorphology 180–181, 180–186.
Trappmann, D., Corona, C., Stoffel, M., 2013. Rolling stones and tree rings: a state of research on dendrogeomorphic reconstructions of rockfall. Prog. Phys. Geogr. 37, 701–716.
Van Den Eeckhaut, M., Muys, B., Loy, K.V., Poesen, J., Beeckman, H., 2009. Evidence for repeated re-activation of old landslides under forest. Earth Surf. Process. Landforms 34, 352–365.
Weber, D., 1994. Research into earth movements in the Barcelonnette basin. In: Casale, R., Fantechi, R., Flageollet, J.-C. (Eds.), Temporal Occurrence and Forecasting of Landslides in the European Community, pp. 321–336. Final Report 1.
Williams, P., Jacoby, G., Buckley, B., 1992. Coincident ages of large landslides in Seattle's Lake Washington. Geol. Soc. Am. Abstr. Programs, 90.